

Article

## ***In Vitro* Assessment of Migratory Behavior of Two Cell Populations in a Simple Multichannel Microdevice**

**Mahboubeh Kabiri**<sup>1,2</sup>, **William B. Lott**<sup>1</sup>, **Ehsan Kabiri**<sup>3</sup>, **Pamela J. Russell**<sup>4</sup> and **Michael R. Doran**<sup>1,4,5,\*</sup>

<sup>1</sup> Stem Cell Therapies Laboratory, Queensland University of Technology, Translational Research Institute, Brisbane 4102, Australia;

E-Mails: m45\_kabiri@yahoo.com (M.K.); b.lott@qut.edu.au (W.B.L.)

<sup>2</sup> Department of Biotechnology, College of Science, University of Tehran, Tehran, Iran

<sup>3</sup> Department of Mechanical Engineering, Esfahan University of Technology, Esfahan, Iran;

E-Mail: ehsan\_kabiri\_33@yahoo.com

<sup>4</sup> Australian Prostate Cancer Research Centre, Translational Research Institute, Brisbane 4102, Australia; E-Mail: pamela.russell@qut.edu.au

<sup>5</sup> Mater Medical Research Institute, Translational Research Institute, Brisbane 4102, Australia

\* Author to whom correspondence should be addressed; E-Mail: michael.doran@qut.edu.au; Tel.: +61-7-3443-7348; Fax: +61-7-3443-7779.

Received: 22 July 2013; in revised form: 17 October 2013 / Accepted: 20 November 2013 /

Published: 18 December 2013

---

**Abstract:** Recent literature suggests that mesenchymal stem/stromal cells (MSC) could be used as Trojan Horses to deliver “death-signals” to cancer cells. Herein, we describe the development of a novel multichannel cell migration device, and use it to investigate the relative migration rates of bone marrow-derived MSC and breast cancer cells (MCF-7) towards each other. Confluent monolayers of MSC and MCF-7 were established in adjacent chambers separated by an array of 14 microchannels. Initially, culture chambers were isolated by air bubbles (air-valves) contained within each microchannel, and then bubbles were displaced to initiate the assay. The MCF-7 cells migrated preferentially towards MSC, whilst the MSC did not migrate preferentially towards the MCF-7 cells. Our results corroborate previous literature that suggests MSC migration towards cancer cells *in vivo* is in response to the associated inflammation rather than directly to signals secreted by the cancer cells themselves.

**Keywords:** cancer cells; MSC migration; multichannel microdevice; paracrine signaling

---

## 1. Introduction

The inability to specifically target cancer cells is a significant limitation of many cancer therapies, and this results in systemic off-target toxicities [1,2]. Mesenchymal stem/stromal cells (MSC) are multipotent stromal cells with the ability to self renew and differentiate into cells of diverse lineage [3]. Their hypoimmunogenicity, ease of isolation, and ease of *ex-vivo* modification have made them increasingly attractive candidates for cell-based therapies. Such MSC-based therapies have traditionally aimed to exploit the differentiation potential and/or the paracrine secretions of transplanted MSC populations to promote tissue repair and regeneration or to dampen inflammatory processes [4,5]. In studies where MSC were infused into healthy animals, MSC largely homed to, or became lodged in, highly vascularized tissues such as the lungs, liver and bones [6–9]. However, in animal models involving tissue injury, MSC appeared to home selectively to the sites of injury and/or the associated inflammation [10–12]. Tumor stroma has been described as “wounds that never heal”, and similarly it appears that MSC home to cancer lesions [13,14]. Based on the premise that MSC selectively home to cancer lesions, MSC theoretically could be utilized to specifically deliver “death-signals” to cancer cells [15–19].

The development of MSC-based delivery therapies will require precise characterization of MSC’s propensity to migrate to cancer cell populations and then specifically unload their “death-signal” payload. We utilized breast cancer epithelial cells (MCF-7) [20] as a model cell line to better characterize the migration behavior of bone marrow-derived MSC towards cancer cell populations. MSC populations migrate towards breast cancers *in vivo* [21]. *In vitro* MSC migrate towards medium conditioned by the more aggressive MCF-7/Ras mutant cells. This *in vitro* study utilized a Transwell™ (Tewksbury, MA, USA) assay to investigate the migration of MSC populations in response to MCF-7/Ras mutant conditioned medium. Whilst the Transwell™ is a robust cell migration platform embraced by the cell culture community, a source-sink microchannel migration device might be more informative, as a more robust gradient could be assured and cell migration could easily be monitored visually in real-time.

In source-sink migration platforms, two large volume reservoirs are connected by a microchannel that enables diffusion between the reservoirs and establishes a gradient within the microchannel. The microchannel dimensions limit diffusive flux from one reservoir to the other, which delays the depletion of chemotactic signal molecules in the source reservoir and the accumulation of these molecules in the sink. This system maintains a reasonably stable gradient across the length of the microchannel, allowing the study of cell migration in response to the signal gradient generated between the two reservoirs.

Source-sink microchannel devices have been previously described (reviewed in [22]), and commercial devices are also available (*i.e.*,  $\mu$ -Slide Chemotaxis, Ibidi GmbH, Planegg, Germany). Both the published devices and the commercial products establish a cell population within the microchannel itself, and then different chemo-attractants or controls are placed into the opposing reservoirs. This configuration generates a chemical gradient directly over the cell population. Neither

the Transwell™ system nor the existing microchannel platforms are appropriate to observe the migration of two different cell populations towards each other.

Our system is a novel variation on the classic source-sink design that enables the observation of two cell populations migrating towards each other in response to the secretions emanating from the opposing cell populations. We used soft lithography to construct a device with two opposing reservoirs that are connected by an array of 14 microchannels. Each microchannel was initially occupied by an air bubble that functioned as a valve (air-valve) to isolate the two cell populations. Monolayers of MSC and cancer cell populations were established in opposing reservoirs, respectively. After overnight incubation, and visual confirmation that confluent monolayers had been established up to the edge of the air-filled microchannels, the air in the air-valves was displaced by briefly creating an air pressure differential across the microchannels. This action effectively established the source-sink configuration by creating continuous media contact between the two culture reservoirs. The medium on each side was then exchanged with fresh medium, and the migration of MSC and MCF-7 cells towards each other was monitored via microscopy.

## 2. Experimental Section

### 2.1. Cell Isolation and Culture

MCF-7 cells were cultured in DMEM/F12 (Gibco, Grand Island, NY, USA) medium supplemented with 5% fetal bovine serum (FBS; Hyclone, Logan, UT, USA) and 1% penicillin/streptomycin (P/S; Gibco, Grand Island, NY, USA). MCF-7 cells were passaged at 80% confluence.

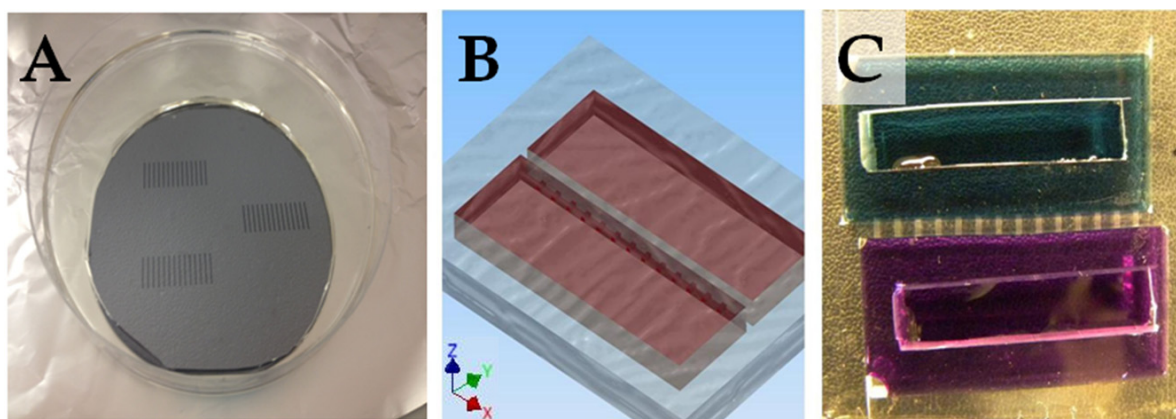
Human MSC isolation and expansion: Approximately 10 mL of bone marrow aspirate were taken from the iliac crest of fully informed healthy volunteer donors in the Mater hospital (Brisbane, Australia). Ethical approval for this study was granted through the Mater Health Services Human Research Ethics Committee and the Queensland University of Technology in accordance with the Australian National Health and Medical Research Council's Statement on Ethical Conduct in Research Involving Humans. Samples were diluted with phosphate-buffered saline (PBS) and mononuclear cells were enriched via density gradient centrifugation as described previously [23,24]. MSC were expanded in low-glucose DMEM (Gibco) containing 10% FBS and 1% P/S, and then sub-cultured in DMEM/F12 supplemented with 5% FBS and 1% P/S for one passage prior to use in migration assays to enable cell adaption to the base medium used in the MCF-7 monocultures and planned migration assays. MSC were used at passages 2 to 4.

### 2.2. Device Fabrication

Figure 1 depicts the design and dimensions of the microchannel migration device. Figure 1A shows the silica wafer (100 mm diameter) used to cast the bodies of three microchannel migration devices simultaneously. The features on the silicon wafer (3 groups of 14 rectangular features, each 1 mm long, 500 µm wide, and 100 µm in height) were formed using SU-8 photo resist (SU8-2025, MicroChem, Newton, MA, USA) as per the manufacturer's instructions (and as described previously) [25]. A 4 mm deep layer of polydimethylsiloxane (PDMS, Sylgard, Dow Corning, Midland, TX, USA) was poured over the wafer surface and cured at 80 °C for 30 min. The cast

patterned PDMS was removed from the silicon wafer and trimmed to make two opposing reservoirs for cell culture as shown in Figure 1B. The PDMS shaped device was then plasma treated for 30 s (high frequency plasma generator Model BD-20, Electro-Technic Products, Chicago, IL, USA), and bonded to a 2 mm thick sheet of glass (Proscitech, Brisbane, Australia) and then placed on a hot plate (80 °C) overnight.

**Figure 1.** Cell migration device. (A) The arrays of 14 microchannels are formed by casting polydimethylsiloxane (PDMS) over channel features on a silica wafer; (B) The resulting device has two reservoirs connected via an array of 14 microchannels; (C) Each reservoir can be filled with medium, whilst filling of the microchannels and mixing between the two reservoirs is initially prevented by the “air-valves”.



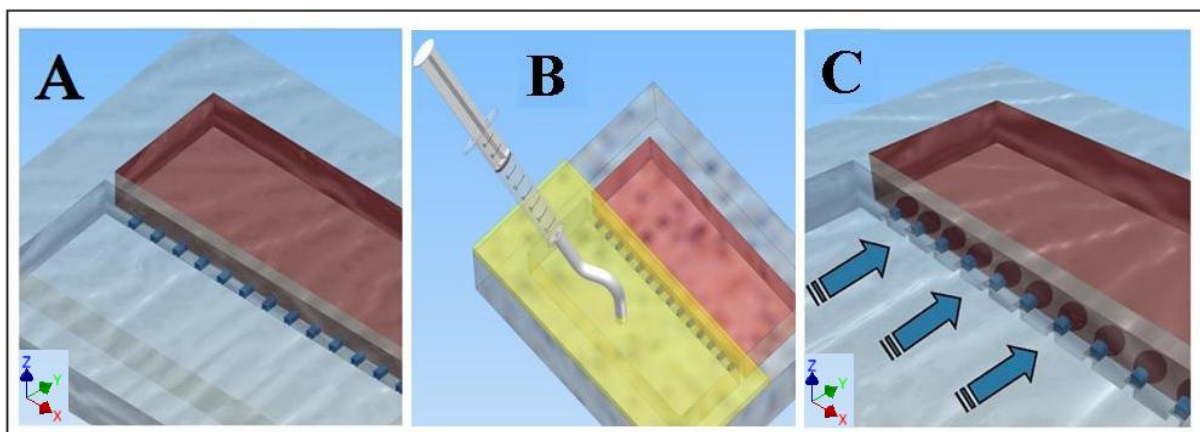
Prior to use, the device was left dry at room temperature for at least two days. Over this time the plasma treated PDMS surface became hydrophobic once again [26]. This is a necessary step, as the microchannels must be hydrophobic for the device to function. The device was sterilized by immersion in 70% ethanol for 2 h, with care to ensure that the ethanol solution entered the microchannels. When necessary, a syringe with needle was used to displace air bubbles. Following sterilization, the ethanol solution was removed, and the device was left in an open sterile petri dish in a biosafety cabinet for two days to dry. Again, it is important that the PDMS surface is not wetted by the ethanol solution prior to use.

### 2.3. Loading the Cell Migration Device

To establish opposing monolayer cell populations, or control medium volumes, 1 mL of cell suspension and/or control media was pipetted into the appropriate reservoirs. For MCF-7 cells, suspensions of 500,000 cells mL<sup>-1</sup> were loaded, whilst for MSC, 60,000 cells mL<sup>-1</sup> were loaded via pipette. The difference in cell seeding densities reflects the relative spread area of the individual cell types and the cell numbers required to generate a confluent monolayer. Each reservoir was loaded in rapid succession to ensure that the air bubbles were trapped within the microchannels (Figure 1C). The hydrophobic nature of the material creates surface tension in the medium that deters immediate medium flow into the small cross-sectional opening of the microchannels. Once both reservoirs were filled with medium, the air bubbles in the microchannels were trapped, and the air-valve was stabilized. Thus, cell attachment and the formation of a monolayer were restricted to the respective

reservoirs, and cells and media were excluded from entering the microchannels. Once cell monolayers were established by overnight incubation, the air bubbles were displaced from the microchannels to create a source-sink configuration. Bubbles were displaced from the microchannels by gently increasing the air pressure disproportionately over one of the reservoirs, thus forcing flow into the opposing chamber (Figure 2). This action was performed using a custom PDMS lid, made freshly before use to enhance adhesiveness, which was fitted with a tube connected to an air-filled syringe over one of the reservoirs, and then gently expelling air from the syringe. The lid was a rectangular PDMS piece large enough to cover the whole reservoir surface. As both the lid and migration device were fabricated from PDMS they formed a strong, but reversible, electrostatic seal. Once a seal had been formed, approximately 1 mL of air was expelled from the syringe to displace the bubbles in the microchannels.

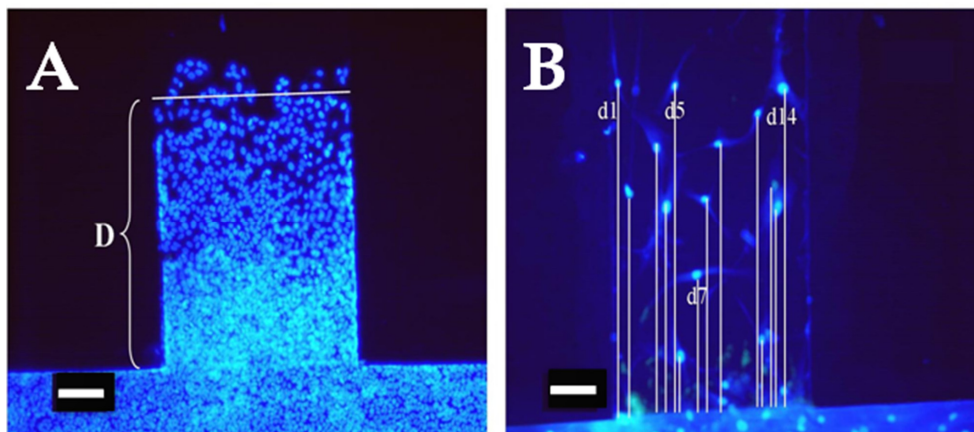
**Figure 2.** (A) Air-valves initially isolate the two reservoirs, preventing fluid flow and cell migration into the microchannels; (B) Using a custom lid, connected to an air-filled syringe, the air pressure over one reservoir was increased slightly; (C) The increase in relative head pressure pushed the light blue fluid into the microchannels and displaced the air bubbles, resulting in a continuous fluidic connection between the two reservoirs.



#### 2.4. Assessing Cell Migration

Immediately following displacement of the air bubbles from the microchannels, the medium in each reservoir was exchanged with fresh medium of the appropriate composition. Time zero phase contrast images were recorded (Nikon Eclipse TE2000-U microscope, Nikon Coolpix 4500 camera (not shown); Tokyo, Japan) Migration cultures were returned to the incubator (37 °C, 5% CO<sub>2</sub>), and phase contrast images were recorded again at days 1, 3 and 5. Parallel cultures were also terminated, cells were fixed in 4% paraformaldehyde and nuclei stained with DAPI (Sigma, St. Louis, MO, USA) Fluorescent images were recorded using the previously described microscope, and cell migration distances were quantified using Image J software (Version #1.47; NIH: Bethesda, MD, USA) Cell migration was characterized by measuring the distance of the cell wave-front in the microchannels from the edge of the channel for cancer cell lines, and by averaging the migrated distance of each single cell inside the channel for MSC populations (see Figure 3). Tracking the movement of individual MSC was required, as MSC did not migrate as a uniform multi-cellular wave-front.

**Figure 3.** Characterization and quantification of cell migration down the microchannels. (A) MCF-7 cells migrate as a wave front down the microchannels. The distance from the microchannel edge “D” is estimated as the distance from the corner of the channel to the average position of the wave front; (B) Mesenchymal stem/stromal cells (MSC) migration is estimated by tracking the distance travelled by individual cells as MSC do not generate a uniform wave front. Scale bar = 100  $\mu\text{m}$ .



### 2.5. Cell Migration Study Design

In all cases the migration of MCF-7 cells and MSC towards each other was quantified, whilst also quantifying the migration of cells towards cell-free medium of similar serum supplementation (5% FBS = negative control), and cell-free medium supplemented with double the serum content (10% FBS = positive control). Although it is possible to conduct similar experiments where the negative control and culture medium are both serum-free, we favored maintaining a serum fraction in all cultures, as serum deprivation is known to dramatically influence cell behavior [27].

## 3. Results and Discussion

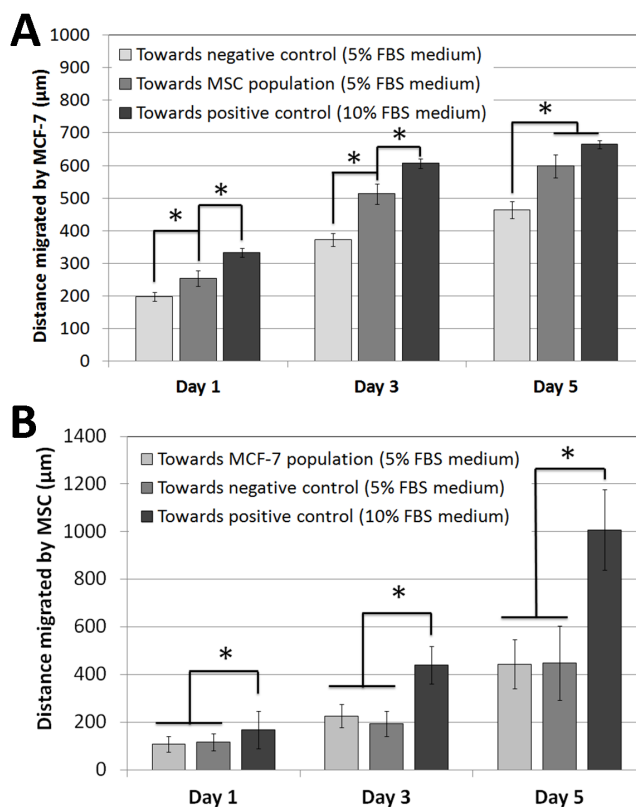
### 3.1. Cell Migration Experiments

Figure 3A,B show the migration of MCF-7 cells and MSC, respectively, through a microchannel and illustrate how migration distances were estimated. The migration behavior of the two cell types differed dramatically, with MCF-7 cells moving as a communal wave front, and MSC migrating independently.

The migration of MCF-7 cells and MSC towards each other, towards equivalent control medium, and towards medium supplemented with 10% FBS was quantified (Figure 4A). Over the first 24 h, MCF-7 cell migration rates towards medium of higher serum content (10% FBS) were greater than towards MSC populations or towards control medium (5% FBS). However, at day 3 and day 5, migration rates towards MSC and higher serum content medium were similar, and with both rates statistically greater ( $p < 0.05$ ) than towards control medium. Maximal MCF-7 wave front migration was observed between day 1 and day 3, and was estimated to be  $137 \pm 26 \mu\text{m}$  per day. The migration of MSC populations towards medium of higher serum content was significantly greater than towards either control medium or towards MCF-7 cell cultures (Figure 4B,  $p < 0.05$  for day 1 and  $p < 10^{-7}$  for

days 3 and 5). The migration rate of MSC towards higher serum content medium was estimated to be  $210 \pm 29 \mu\text{m}$  per day. In contrast, the migration rates of MSC towards MCF-7 populations and control medium were similar, but significantly slower than towards the serum-rich control medium (estimated to be  $84 \pm 14$  and  $83 \pm 19 \mu\text{m}$  per day). Thus, MSC populations did not demonstrate preferential active migration towards MCF-7 cell cultures, unlike the MCF-7 populations, which did actively migrate towards MSC cultures.

**Figure 4.** Quantification of MCF-7 and MSC migration. (A) At Day 1, MCF-7 migration towards higher serum content medium was greatest, whilst at Days 3 and 5, migration towards MSC and higher serum content medium was greater than towards control medium; (B) At all days, MSC migration towards higher serum content medium is greater than towards control medium or MCF-7 cultures ( $n = 14$ , error bars = one standard error of the mean, \* indicates  $p < 0.05$ ).



Herein, we describe the fabrication and operation of a novel cell migration device, and use it to characterize MCF-7 breast cancer epithelial cells and bone marrow-derived MSC migration towards each other in interesting source-sink type assays. Various microchannel devices have been used in studies regarding the migration of cancer cells and other cell types [28,29], however the unique feature of the presented device is its array of 14 microchannels that connects source and sink culture reservoirs. During set-up, the entry of cells and/or culture medium into the microchannels was prevented by air bubbles (air-valves) that occupied each hydrophobic microchannel. Once monolayer cultures had been established in the isolated reservoirs, the air-valve bubbles were displaced, connecting the source and sink via the microchannel array. Various source-sink configurations were

used to determine if MCF-7 populations or MSC populations preferentially migrated towards each other relative to media having varying serum supplementation.

Our results indicated that MCF-7 cells actively migrated both towards higher FBS concentrations and towards MSC populations (Figure 4A). This result is rational given the wealth of published data demonstrating that MSC populations secrete a number of chemokines including CXC ligand 12 (CXCL12), CX3CL1, CXCL16, CC chemokine ligand 3 (CCL3), and CCL19 [30]. Among these CXCL12 plays a pivotal role in modulation of mobilization and homing of different cell types [31]. Breast cancer cells are known to respond to CXCL12 [32–35]. The MCF-7 cell response to MSC paracrine signals is also consistent with recent published data indicating that MSC secretions may play a key role in tumor development *in vivo* [21,36]. Contrary to the concept that MSC might be used to combat cancer, evidence suggests that MSC can support further tumor progression when infused into animal models by supporting the growth of cancer and possibly cancer stem cells [21]. The result may depend on the particular microenvironment in which the cells are found as well as on the chemokine pairing between different cell types within that environment. Cumulatively, these reports suggest that MCF-7 would respond to MSC paracrine signals. The migration device we describe here might be useful in characterizing cancer cell responses to the various panels of MSC secretions.

MSC have been reported to migrate towards cancer lesions *in vivo* [14,18,37–40], and *in vitro* studies have shown that MSC actively migrate towards the MCF-7/Ras mutant cells [21]. Stem cells derived from adipose tissue also actively migrate towards breast cancer cells *in vitro*, likely as a response to tumor cell-derived platelet-derived growth factor BB (PDGF-BB) [41]. However, our results in Figure 4B indicate that bone marrow-derived MSC populations do not necessarily preferentially migrate towards MCF-7 cells *in vitro*. MSC migration within cancer lesions is believed to be largely in response to the localized inflammatory response [42], and *in vitro* cultures do not accurately mimic an inflammatory response. Therefore, it may not be logical to expect MSC to migrate towards MCF-7 cells *in vitro*. Nevertheless, the rationalization that MSC may migrate only in response to paracrine signals generated by immune cells prompts us to query if “death-signals” can be expected to reach their intended destination, or will they more likely be delivered to these by-stander immune cells? Additionally, will an alternative and perhaps unappreciated inflammatory response elsewhere in the body simply divert delivered MSC from their intended path? These are interesting questions that are beyond the scope of this paper, but we believe that improved migration assays like the one described here will facilitate characterization of cell migration behavior in response to chemotactic gradients.

#### 4. Conclusions

In summary, we have outlined a novel microchannel cell migration device that enables quantification of cell population migration toward each other. Using this system we show that MCF-7 cells actively migrate towards MSC populations, but that MSC do not actively migrate towards MCF-7 populations *in vitro*.

#### Conflicts of Interest

The authors declare no conflicts of interest.

## References

1. Lima, F.R.; Kahn, S.A.; Soletti, R.C.; Biasoli, D.; Alves, T.; da Fonseca, A.C.C.; Garcia, C.; Romão, L.; Brito, J.; Holanda-Afonso, R.; *et al.* Glioblastoma: Therapeutic challenges, What lies ahead. *Biochim. Biophys. Acta* **2012**, *1826*, 338–349.
2. Huang, T.T.; Sarkaria, S.M.; Cloughesy, T.F.; Mischel, P.S. Targeted therapy for malignant glioma patients: Lessons learned and the road ahead. *Neurotherapeutics* **2009**, *6*, 500–512.
3. Pittenger, M.F.; Mackay, A.M.; Beck, S.C.; Jaiswal, R.K.; Douglas, R.; Mosca, J.D.; Moorman, M.A.; Simonetti, D.W.; Craig, S.; Marshak, D.R. Multilineage potential of adult human mesenchymal stem cells. *Science* **1999**, *284*, 143–147.
4. English, K.; French, A.; Wood, K.J. Mesenchymal stromal cells: Facilitators of successful transplantation? *Cell Stem Cell* **2010**, *7*, 431–442.
5. Si, Y.L.; Zhao, Y.L.; Hao, H.J.; Fu, X.B.; Han, W.D. MSCs: Biological characteristics, clinical applications and their outstanding concerns. *Ageing Res. Rev.* **2011**, *10*, 93–103.
6. Herzog, E.L.; van Arnem, J.; Hu, B.; Zhang, J.; Chen, Q.; Haberman, A.M.; Krause, D.S. Lung-specific nuclear reprogramming is accompanied by heterokaryon formation and Y chromosome loss following bone marrow transplantation and secondary inflammation. *FASEB J.* **2007**, *21*, 2592–2601.
7. Weiss, D.J.; Bertoncello, I.; Borok, Z.; Kim, C.; Panoskaltsis-Mortari, A.; Reynolds, S.; Rojas, M.; Stripp, B.; Warburton, D.; Prockop, D.J. Stem cells and cell therapies in lung biology and lung diseases. *Proc. Am. Thorac. Soc.* **2011**, *8*, 223–272.
8. Albera, C.; Polak, J.; Janes, S.; Griffiths, M.; Alison, M.; Wright, N.; Navaratnarasah, S.; Poulson, R.; Jeffery, R.; Fisher, C.; *et al.* Repopulation of human pulmonary epithelium by bone marrow cells: A potential means to promote repair. *Tissue Eng.* **2005**, *11*, 1115–1121.
9. Barbash, I.M.; Chouraqui, P.; Baron, J.; Feinberg, M.S.; Etzion, S.; Tessone, A.; Miller, L.; Guetta, E.; Zipori, D.; Kedes, L.H.; *et al.* Systemic delivery of bone marrow—Derived mesenchymal stem cells to the infarcted myocardium. *Circulation* **2003**, *108*, 863–868.
10. Lee, R.H.; Seo, M.J.; Reger, R.L.; Spees, J.L.; Pulin, A.A.; Olson, S.D.; Prockop, D.J. Multipotent stromal cells from human marrow home to and promote repair of pancreatic islets and renal glomeruli in diabetic NOD/scid mice. *Proc. Natl. Acad. Sci. USA* **2006**, *103*, 17438–17443.
11. Hara, M.; Murakami, T.; Kobayashi, E. *In vivo* bioimaging using photogenic rats: Fate of injected bone marrow-derived mesenchymal stromal cells. *J. Autoimmun.* **2008**, *30*, 163–171.
12. Chapel, A.; Bertho, J.M.; Bensidhoum, M.; Fouillard, L.; Young, R.G.; Frick, J.; Demarquay, C.; Cuvelier, F.; Mathieu, E.; Trompier, F.; *et al.* Mesenchymal stem cells home to injured tissues when co-infused with hematopoietic cells to treat a radiation-induced multi-organ failure syndrome. *J. Gene Med.* **2003**, *5*, 1028–1038.
13. Plytycz, B.; Seljelid, R. From inflammation to sickness: Historical perspective. *Arch. Immunol. Ther. Exp. (Warsz)* **2003**, *51*, 105–109.
14. Houghton, J.M.; Morozov, A.; Smirnova, I.; Wang, T.C. Stem cells and cancer. *Semin. Cancer Biol.* **2007**, *17*, 191–203.
15. Loebinger, M.R.; Eddaoudi, A.; Davies, D.; Janes, S.M. Mesenchymal stem cell delivery of TRAIL can eliminate metastatic cancer. *Cancer Res.* **2009**, *69*, 4134–4142.

16. Kanehira, M.; Xin, H.; Hoshino, K.; Maemondo, M.; Mizuguchi, H.; Hayakawa, T.; Matsumoto, K.; Nakamura, T.; Nukiwa, T.; Saijo, Y. Targeted delivery of NK4 to multiple lung tumors by bone marrow-derived mesenchymal stem cells. *Cancer Gene Ther.* **2007**, *14*, 894–903.
17. Chen, X.; Lin, X.; Zhao, J.; Shi, W.; Zhang, H.; Wang, Y.; Kan, B.; Du, L.; Wang, B.; Wei, Y.; *et al.* A tumor-selective biotherapy with prolonged impact on established metastases based on cytokine gene-engineered MSCs. *Mol. Ther.* **2008**, *16*, 749–756.
18. Ren, C.; Kumar, S.; Chanda, D.; Chen, J.; Mountz, J.D.; Ponnazhagan, S. Therapeutic Potential of Mesenchymal Stem Cells Producing Interferon- $\alpha$  in a Mouse Melanoma Lung Metastasis Model. *Stem Cells* **2008**, *26*, 2332–2338.
19. Tang, C.; Russell, P.J.; Martiniello-Wilks, R.; Rasko, J.E.; Khatri, A. Concise review: Nanoparticles and cellular carriers-allies in cancer imaging and cellular gene therapy? *Stem Cells* **2010**, *28*, 1686–1702.
20. Bacus, S.S.; Kiguchi, K.; Chin, D.; King, C.R.; Huberman, E. Differentiation of cultured human breast cancer cells (AU-565 and MCF-7) associated with loss of cell surface HER-2/neu antigen. *Mol. Carcinogen.* **1990**, *3*, 350–362.
21. Karnoub, A.E.; Dash, A.B.; Vo, A.P.; Sullivan, A.; Brooks, M.W.; Bell, G.W.; Richardson, A.L.; Polyak, K.; Tubo, R.; Weinberg, R.A. Mesenchymal stem cells within tumour stroma promote breast cancer metastasis. *Nature* **2007**, *449*, 557–563.
22. Chung, B.G.; Choo, J. Microfluidic gradient platforms for controlling cellular behavior. *Electrophoresis* **2010**, *31*, 3014–3027.
23. Kabiri, M.; Kul, B.; Lott, W.; Futrega, K.; Ghanavia, P.; Upton, Z.; Doran, M. 3D mesenchymal stem/stromal cell osteogenesis and autocrine signalling. *Biochem. Biophys. Res. Commun.* **2012**, *419*, 142–147.
24. Markway, B.D.; Tan, G.K.; Brooke, G.; Hudson, J.E.; Cooper-White, J.J.; Doran, M.R. Enhanced chondrogenic differentiation of human bone marrow-derived mesenchymal stem cells in low oxygen environment micropellet cultures. *Cell Transplant.* **2010**, *19*, 29–42.
25. Doran, M.R.; Mills, R.J.; Parker, A.J.; Landman, K.A.; Cooper-White, J.J. A cell migration device that maintains a defined surface with no cellular damage during wound edge generation. *Lab Chip.* **2009**, *9*, 2364–2369.
26. Bodas, D.; Khan-Malek, C. Hydrophilization and hydrophobic recovery of PDMS by oxygen plasma and chemical treatment—An SEM investigation. *Sens. Actuators B* **2007**, *123*, 368–373.
27. Egeblad, M.; Jaattela, J. Cell death induced by TNF or serum starvation is independent of ErbB receptor signaling in MCF-7 breast carcinoma cells. *Int. J. Cancer* **2000**, *86*, 617–625.
28. Chen, S.-H.; Hung, W.-C.; Wang, P.; Paul, C.; Konstantopoulos, K. Mesothelin Binding to CA125/MUC16 Promotes Pancreatic Cancer Cell Motility and Invasion via MMP-7 Activation. *Sci. Rep.* **2013**, *3*, doi:10.1038/srep01870.
29. Irimia, D.; Toner, M. Spontaneous migration of cancer cells under conditions of mechanical confinement. *Integrat. Biol.* **2009**, *1*, 506–512.
30. Sordi, V.; Malosio, M.L.; Marchesi, F.; Mercalli, A.; Melzi, R.; Giordano, T.; Belmonte, N.; Ferrari, G.; Leone, B.E.; Bertuzzi, F.; *et al.* Bone marrow mesenchymal stem cells express a restricted set of functionally active chemokine receptors capable of promoting migration to pancreatic islets. *Blood* **2005**, *106*, 419–427.

31. Ryu, C.H.; Park, S.A.; Kim, S.M.; Lim, J.Y.; Jeong, C.H.; Jun, J.A.; Oh, J.H.; Park, S.H.; Oh, W.I.; Jeun, S.S. Migration of human umbilical cord blood mesenchymal stem cells mediated by stromal cell-derived factor-1/CXCR4 axis via Akt, ERK, and p38 signal transduction pathways. *Biochem. Biophys. Res. Commun.* **2010**, *398*, 105–110.
32. Bachelder, R.E.; Wendt, M.A.; Mercurio, A.M. Vascular endothelial growth factor promotes breast carcinoma invasion in an autocrine manner by regulating the chemokine receptor CXCR4. *Cancer Res.* **2002**, *62*, 7203–7206.
33. Lee, B.C.; Lee, T.H.; Avraham, S.; Avraham, H.K. Involvement of the Chemokine Receptor CXCR4 and Its Ligand Stromal Cell-Derived Factor 1 $\alpha$  in Breast Cancer Cell Migration Through Human Brain Microvascular Endothelial Cells. *Mol. Cancer Res.* **2004**, *2*, 327–338.
34. Hall, J.M.; Korach, K.S. Stromal cell-derived factor 1, a novel target of estrogen receptor action, mediates the mitogenic effects of estradiol in ovarian and breast cancer cells. *Mol. Endocrinol.* **2003**, *17*, 792–803.
35. Müller, A.; Homey, B.; Soto, H.; Ge, N.; Catron, D.; Buchanan, M.E.; McClanahan, T.; Murphy, E.; Yuan, W.; Wagner, S.N.; *et al.* Involvement of chemokine receptors in breast cancer metastasis. *Nature* **2001**, *410*, 50–56.
36. Spaeth, E.L.; Dembinski, J.L.; Sasser, A.K.; Watson, K.; Klopp, A.; Hall, B.; Andreeff, M.; Marini, F. Mesenchymal stem cell transition to tumor-associated fibroblasts contributes to fibrovascular network expansion and tumor progression. *PLoS One* **2009**, *4*, e4992.
37. Stoicov, C.; Li, H.; Carlson, J.; Houghton, J.M. Bone marrow cells as the origin of stomach cancer. *Future Oncol.* **2005**, *1*, 851–862.
38. Corsten, M.F.; Shah, K. Therapeutic stem-cells for cancer treatment: Hopes and hurdles in tactical warfare. *Lancet Oncol.* **2008**, *9*, 376–384.
39. Hall, B.; Dembinski, J.; Sasser, A.K.; Studeny, M.; Andreeff, M.; Marini, F. Mesenchymal stem cells in cancer: Tumor-associated fibroblasts and cell-based delivery vehicles. *Int. J. Hematol.* **2007**, *86*, 8–16.
40. Kim, S.M.; Kim, D.S.; Jeong, C.H.; Kim, D.H.; Kim, J.H.; Jeon, H.B.; Kwon, S.J.; Jeun, S.S.; Yang, Y.S.; Oh, W.; *et al.* CXC chemokine receptor 1 enhances the ability of human umbilical cord blood-derived mesenchymal stem cells to migrate toward gliomas. *Biochem. Biophys. Res. Commun.* **2011**, *407*, 741–746.
41. Gehmert, S.; Prantl, L.; Vykoukal, J.; Alt, E.; Song, Y.H. Breast cancer cells attract the migration of adipose tissue-derived stem cells via the PDGF-BB/PDGFR- $\beta$  signaling pathway. *Biochem. Biophys. Res. Commun.* **2010**, *398*, 601–605.
42. Ben-Baruch, A. The tumor-promoting flow of cells into, within and out of the tumor site: Regulation by the inflammatory axis of TNF $\alpha$  and chemokines. *Cancer Microenviron.* **2012**, 1–14.